Receive Diversity Revisited: Correlation, Coupling and Noise

Carlo P. Domizioli, Brian L. Hughes, Kevin G. Gard and Gianluca Lazzi
Department of Electrical and Computer Engineering
North Carolina State University
Raleigh, NC 27695-7914
{*cpdomizi,blhughes,kevin_gard,lazzi*}@*ncsu.edu*

***Abstract*—Previous studies of receive diversity have carefully modeled the impact of spatial correlation and antenna coupling on the signal component at the receiver. By contrast, relatively little attention has been paid to noise. In this paper we introduce a receive diversity model that articulates the dominant physical noise sources and relates their spatial correlation to the properties of the antennas, front-end amplifiers and matching networks. We then derive an optimal receiver as well as a formula for the resulting outage probability in terms of these noise sources. Numerical results are presented which suggest that different noise sources can impact performance in profoundly different ways.**

I. Introduction

Signal reception in a mobile wireless receiver is impaired by fading – the random power fluctuations that result from constructive and destructive interference of scattered radio waves. Receive diversity is a well-known technique that improves reception by using an antenna array to collect multiple fading signals. The degree of improvement depends on the correlation between the signals – highly correlated signals offer little improvement since they tend to fade simultaneously, while uncorrelated signals offer a large gain since simultaneous fades are highly unlikely. Signal correlation depends on the spatial statistics of the incident electric field, the array radiation pattern and coupling between the antennas.

Lee [1] first investigated the effect of spatial correlation and antenna coupling on receive diversity by representing the antenna array and receiver as multiport networks. He showed that diversity performance was dependent on the antenna terminations and for certain (albeit impractical) terminations, mutual coupling may improve performance. In the decades since this work, there have been numerous studies of correlation and coupling in antenna arrays. This is due to the many applications of antenna arrays, which include reducing co-channel interference [2] and increasing capacity with multiple-input multiple-output (MIMO) systems [3]. MIMO systems in particular have attracted much recent attention [4] - [9].

Previous work on mutual coupling has carefully modeled the impact of coupling on the signal component; however, relatively little attention has been paid to noise. In fact, most of the works cited above do not include detailed models of noise. Instead, noise is modeled as white and Gaussian with a fixed distribution, regardless of its source or the surrounding receiver design. However, real receivers are plagued by diverse noise sources. These sources are affected by antenna coupling, matching networks and amplifiers in different ways. Since the signal and noise play equal roles in determining most system performance metrics, a channel model that does not correctly represent noise cannot be expected to correctly predict performance.

Some recent work has improved the noise modeling in multi-antenna receivers. In [10] a realistic noise model for the front-end amplifiers is introduced and matching networks that optimize power transfer and noise performance are compared for dual diversity. The effect of noise matching on the capacity of MIMO systems for sky-noise-limited and amplifier-noise-limited scenarios was addressed in [11] and [12]. While these studies are a significant step forward from the spatially white noise model, several issues remain to be addressed. First, the optimal receiver for correlated noise and expressions relating the outage probability to the signal and noise correlation have not been developed. Second, most modern front-end amplifiers have low noise figures so no single noise source can be regarded as dominant. There are several significant sources of noise in the receiver that need to be considered.

In this paper we introduce a receive diversity model that articulates the dominant physical noise sources and relates their spatial correlation to the properties of the antennas, front-end amplifiers and matching networks. We derive an optimal receiver for this system as well as an explicit formula for the resulting outage probability in terms of these noise sources. Numerical examples are presented for different noise sources and matching networks. The results suggest that different noise sources can impact performance in profoundly different ways.

II. Receive Diversity with Correlated Noise

When antennas are brought close together, the noise components in each branch may become correlated. In this section, we present an optimal combiner for receive diversity with correlated noise, as well as a formula for the resulting outage probability. The specific form of noise correlation which results from mutual coupling is derived in the next section.

The received signals in an M-branch diversity system with frequency-flat, quasi-static fading may be expressed as

$$\mathbf{r} = \sqrt{\mathcal{E}}\mathbf{h}x + \mathbf{n} \ , \tag{1}$$

[1]This material is based upon work supported by the National Science Foundation under grants CCF-0312686 and CCF-0515164.

1930-529X/07/$25.00 © 2007 IEEE
This full text paper was peer reviewed at the direction of IEEE Communications Society subject matter experts for publication in the IEEE GLOBECOM 2007 proceedings.

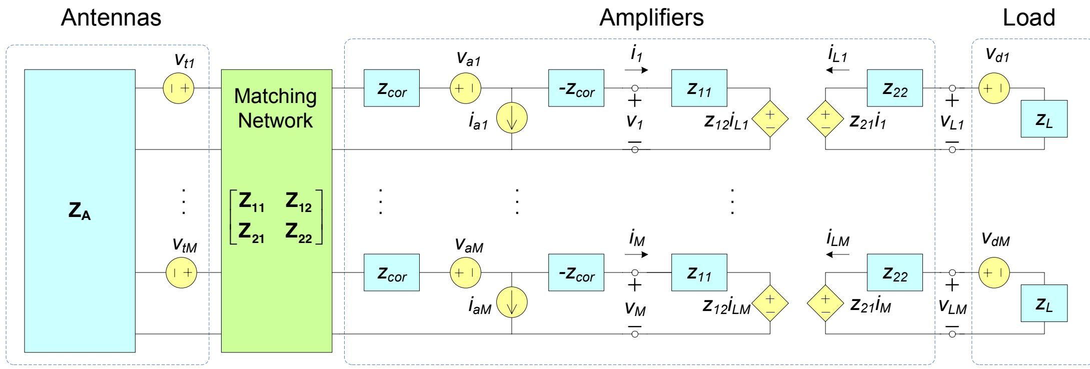

Fig. 1. Circuit model of a post-detection diversity receiver.

where x is a complex information symbol with $\mathrm{E}[|x|^2] = 1$, $\mathrm{E}[\cdot]$ denotes the expectation, $\mathcal{E}$ is the average received energy per branch, $\mathbf{h}$ is an M-dimensional column vector of fading path gains and $\mathbf{n}$ represents noise. We assume $\mathbf{h}$ is a zero-mean, circularly-symmetric complex Gaussian random vector, denoted by $\mathbf{h} \sim \mathcal{CN}(\mathbf{0}, \mathbf{\Sigma_h})$, where $\mathbf{\Sigma_h} = \mathrm{E}[\mathbf{h}\mathbf{h}^H]$ and the superscript H denotes the conjugate-transpose. We also assume that the noise is spatially correlated, so $\mathbf{n} \sim \mathcal{CN}(\mathbf{0}, \mathbf{\Sigma_n})$. Most prior work on receive diversity has assumed spatially white noise.

The receiver employs a linear combiner of the form

$$y = \mathbf{w}^H\mathbf{r} = \tilde{h}x + \tilde{n} \tag{2}$$

where $\tilde{h}x$ represents the signal component and $\tilde{n}$ is the noise. From (1), the instantaneous signal-to-noise ratio (SNR) at the combiner output is then

$$\gamma(\mathbf{w}) \;=\; \frac{|\tilde{h}|^2}{\mathrm{E}[|\tilde{n}|^2]} \;=\; \mathcal{E}\frac{|\mathbf{w}^H\mathbf{h}|^2}{\mathbf{w}^H\mathbf{\Sigma_n}\mathbf{w}} \;. \tag{3}$$

In maximum-ratio combining (MRC), the combiner $\mathbf{w}$ is chosen to maximize $\gamma(\mathbf{w})$. For uncorrelated noise, say $\mathbf{\Sigma_n} = \mathbf{I}$ where $\mathbf{I}$ is the identity matrix, it is well known [13] that $\gamma(\mathbf{w})$ is maximized if and only if the combiner is of the form $\mathbf{w} \propto \mathbf{h}$.

For correlated noise, let $\mathbf{\Sigma}_\mathbf{n}^{\frac{1}{2}}$ denote the Hermitian square-root of $\mathbf{\Sigma_n}$. Observe that the change of variable $\mathbf{u} = \mathbf{\Sigma}_\mathbf{n}^{\frac{1}{2}}\mathbf{w}$ puts (3) in a form similar to the white noise case:

$$\gamma(\mathbf{u}) \;=\; \mathcal{E}\frac{|\mathbf{u}^H\mathbf{\Sigma}_\mathbf{n}^{-\frac{1}{2}}\mathbf{h}|^2}{\mathbf{u}^H\mathbf{u}} \;. \tag{4}$$

It follows that γ is maximized if and only if $\mathbf{u} \propto \mathbf{\Sigma}_\mathbf{n}^{-\frac{1}{2}}\mathbf{h}$, or equivalently $\mathbf{w} \propto \mathbf{\Sigma}_\mathbf{n}^{-1}\mathbf{h}$. The resulting optimal SNR is then[1]

$$\gamma^o \;=\; \max_{\mathbf{w}} \;\gamma(\mathbf{w}) \;=\; \mathcal{E}\cdot\mathbf{h}^H\mathbf{\Sigma}_\mathbf{n}^{-1}\mathbf{h} \;. \tag{5}$$

In particular, note that the conventional MRC is suboptimal for spatially correlated noise.

The performance of receive diversity systems is often measured by the outage probability, defined as

$$P_{\text{out}}(\tau) = \Pr\{\gamma^o \le \tau\} \;, \tag{6}$$

where τ is a non-negative threshold. A closed-form expression for the outage can be obtained using the results of [1]: If $0 < \lambda_1 < \cdots < \lambda_M$ are the distinct positive eigenvalues of $\mathcal{E}\mathbf{\Sigma_h}\mathbf{\Sigma}_\mathbf{n}^{-1}$, then [2]

$$P_{\text{out}}(\tau) = \sum_{j=1}^{M}\frac{\lambda_j^{M-1}\left(1 - e^{-\tau/\lambda_j}\right)}{\prod_{i\neq j}(\lambda_j - \lambda_i)} \;. \tag{7}$$

The outage probability for zero or repeated eigenvalues can also be obtained from [1]. In particular, for $\mathbf{\Sigma_h} = \mathbf{I}$ and $\mathbf{\Sigma_n} = N_0\mathbf{I}$, we recover Brennan's classic outage formula for i.i.d. fading and noise [13]:

$$P_{\text{out}}(\tau) = \frac{1}{(M-1)!}\int_0^{\tau/\Gamma} t^{M-1}e^{-t}dt \;, \tag{8}$$

where $\Gamma = \mathcal{E}/N_0$ is the average SNR.

III. Receiver Model

Consider an M-antenna diversity receiver with mutual coupling and optimal post-detection combining. The output of each antenna is amplified, demodulated and digitized before combining. We assume coupling occurs only between antennas; there is no coupling between the amplifiers, demodulators or A/D converters in each branch. We further assume a narrowband system, so all impedances are approximately constant over the system bandwidth and all signals can be expressed in complex baseband form.

A circuit model of this receiver is illustrated in Fig. 1. This model reflects the impedances of the antenna array, matching network, amplifiers and load as well as the currents and voltages due to the signal and dominant noise sources. Each of these components is described in detail below.

A. Antenna Array

The function of an antenna is to convert an incident electromagnetic field into a voltage across the antenna terminals. When the antennas of an array are closely spaced, the terminal voltage of each antenna depends not only on the field at that antenna but also on the currents flowing through neighboring

[1] Optimization problems of this form are encountered in many other areas; adaptive array processing is one related example [14, pg. 60].

[2] This follows from the Appendix of [1] by writing $\gamma^o = \mathbf{h}_\mathbf{w}^H\mathbf{\Sigma}\mathbf{h}_\mathbf{w}$, where $\mathbf{h}_\mathbf{w} \sim \mathcal{CN}(\mathbf{0}, \mathbf{I})$ and $\mathbf{\Sigma} = \mathcal{E}\mathbf{\Sigma}_\mathbf{h}^{1/2}\mathbf{\Sigma}_\mathbf{n}^{-1}\mathbf{\Sigma}_\mathbf{h}^{1/2}$, and observing that $\mathcal{E}\mathbf{\Sigma_h}\mathbf{\Sigma}_\mathbf{n}^{-1}$ has the same eigenvalues as $\mathbf{\Sigma}$.

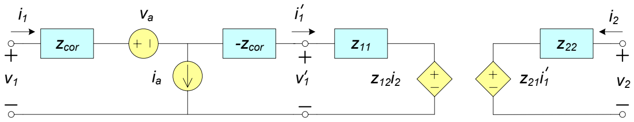

Fig. 2. The Rothe-Dahlke model of an amplifier.

antennas. At the system design level, we can represent the array as an M-port Thevenin equivalent circuit, as shown in Fig. 1. The relationship between terminal voltages and currents is then described by an $M \times M$ impedance matrix $\mathbf{Z_A}$, where $[\mathbf{Z_A}]_{ii}$ is the self-impedance of antenna i and $[\mathbf{Z_A}]_{ij}$ is the mutual impedance between antennas i and j. Approximate formulas for these impedances are available for thin dipoles [15, ch. 8]; other types of antennas may be evaluated by numerical techniques.

The open-circuit antenna voltage $\mathbf{V}_t$ represents the combined effects of both signal and noise in the array, and can be written as

$$\mathbf{V}_t = \sqrt{\mathcal{E}}\mathbf{h_t}x + \mathbf{n_t} \tag{9}$$

where $\sqrt{\mathcal{E}}\mathbf{h_t}x$ is the voltage induced by the incident signal electric field. As in the previous section, we assume $\mathbf{h_t} \sim \mathcal{CN}(\mathbf{0}, \mathbf{\Sigma_{h_t}})$. For perfectly conducting antennas, $\mathbf{n_t}$ is the voltage induced in the array by noise sources in the surrounding environment. These sources may include thermal radiation, cosmic background radiation and interference from other electronic devices. We consider the canonical example of thermal radiation from a spherically isotropic distribution of black-body radiators [16, pg. 111] at uniform temperature T_0. The noise voltage is then $\mathbf{n_t} \sim \mathcal{CN}(\mathbf{0}, \mathbf{\Sigma_{n_t}})$, where the correlation matrix is given by Twiss [17] [3]

$$\mathbf{\Sigma_{n_t}} = 2kT_0B(\mathbf{Z_A} + \mathbf{Z_A}^H) \ , \tag{10}$$

$k = 1.38 \times 10^{-23}$ J/K is Boltzmann's constant and B is the system bandwidth in Hz. In this paper, we take $T_0 = 290$ K, the standard temperature. For large inter-element spacings, note that $\mathbf{Z_A}$ is essentially diagonal and so the noise is spatially white. For spacings less than a few wavelengths, however, $\mathbf{Z_A}$ is not diagonal and the noise is correlated. Since correlated noise is generally desirable in communications, we expect that neglecting this correlation in previous analyses will yield overly pessimistic performance estimates. We will illustrate this point later with an example.

B. Amplifiers

An amplifier is usually well-modeled (within its dynamic range) as a linear, noisy two-port network. According to Rothe and Dahlke [18], any such network can be represented by a simple noise network cascaded with a noise-free network, as shown in Fig. 2. The noise voltage v_a and current i_a are independent zero-mean Gaussian RVs which model some combination of thermal and shot noise generated by internal elements. A common convention is to normalize the variances of these sources by the thermal noise power generated by a 1 Ω resistor at standard temperature. Thus, the *equivalent noise resistance* of the voltage source and the *equivalent noise conductance* of the current source are given respectively by

$$r_a = \frac{\mathrm{E}\left[|v_a|^2\right]}{4kT_0B} \ , \ g_a = \frac{\mathrm{E}\left[|i_a|^2\right]}{4kT_0B}. \tag{11}$$

The parameter $z_{cor} = r_{cor} + jx_{cor}$, called the *correlation impedance*, reflects the degree of correlation between the noise observed at the two output terminals. The noise statistics of an amplifier are completely characterized by $\{r_a, g_a, z_{cor}\}$.

An important amplifier metric is the *noise factor*, F, defined as the ratio of the output noise power to the noise power contributed by a source alone, when a source impedance $z_s = r_s + jx_s$ at standard temperature is connected to the input port, i.e.,

$$F = \frac{\mathrm{E}\left[|v_2|^2\right]}{\mathrm{E}\left[|v_2|^2\right]\big|_{v_a=i_a=0}} = 1 + \frac{1}{r_s}\left(r_a + g_a\left|z_s + z_{cor}\right|^2\right).$$

The noise factor is useful because it relates the input and output SNRs of the amplifier, given in dB by $\mathrm{SNR}_{\mathrm{out}} = \mathrm{SNR}_{\mathrm{in}} - \mathrm{NF}$, where $\mathrm{NF} = 10\log_{10} F$ is the *noise figure*.

Note that F attains its minimum value F_{min} when $z_s = z_{opt}$ where [18]

$$F_{min} = 1 + 2\left(g_a r_{cor} + \sqrt{g_a r_a + (g_a r_{cor})^2}\right) \tag{12}$$

$$z_{opt} = \sqrt{r_a/g_a + r_{cor}^2} - jx_{cor}. \tag{13}$$

This defines a new set of noise parameters, $\{F_{min}, g_a, z_{opt}\}$, which are typically used in low-noise amplifier (LNA) design.[4]

C. Load

Since the receiver chains downstream from the amplifiers are assumed to be electrically isolated from one another, the noise in each branch is independent and the impedances are uncoupled. The downstream components consist of filters, mixers, amplifiers and other analog circuits that generate a combination of thermal and shot noise and possibly other varieties of noise that are inherent to each device. Here we reference the total downstream noise to the amplifier output and simply assume that each branch may be modeled by an impedance z_L and a zero-mean Gaussian noise voltage v_{di} with equivalent noise resistance r_d.

D. Matching Network

Matching networks are often used to alter the source (array) impedance, usually in order to maximize power transfer or minimize the noise factor. Ideally the network is formed with passive, reactive elements so it is noiseless, lossless and reciprocal. The matching network in Fig. 1 has M input and output ports. If $\mathbf{V}_i, \mathbf{I}_i, \mathbf{V}_o, \mathbf{I}_o$ denote the voltages and currents at the input and output of the device, respectively, then

$$\begin{aligned} \mathbf{V}_i &= \mathbf{Z_{11}}\mathbf{I}_i + \mathbf{Z_{12}}\mathbf{I}_o \\ \mathbf{V}_o &= \mathbf{Z_{21}}\mathbf{I}_i + \mathbf{Z_{22}}\mathbf{I}_o \end{aligned}$$

[3] An elegant, alternative derivation was recently given by Gans [11].

[4] A variation of these parameters based on the admittance version of the Rothe-Dahlke model are $\{F_{min}, R_n, Y_{opt}\}$. For microwave amplifiers a reflection coefficient Γ_{opt} is usually given in place of Y_{opt} [20, pg. 558].

It can be shown [19, pg. 13] that the network is lossless (no power is dissipated within it) provided the following conditions are satisfied: $\mathbf{Z_{11}} = -\mathbf{Z_{11}^H}$, $\mathbf{Z_{22}} = -\mathbf{Z_{22}^H}$, $\mathbf{Z_{21}} = -\mathbf{Z_{12}^H}$. From the standpoint of the rest of the receiver, the antennas plus matching comprise a noisy linear network which can be represented by a Thevenin equivalent circuit with

$$\begin{aligned} \mathbf{V}'_t &= \mathbf{M}\mathbf{V}_t \ , \ \mathbf{M} \ = \ \mathbf{Z_{21}}(\mathbf{Z_{11}} + \mathbf{Z_A})^{-1} \\ \mathbf{Z}'_\mathbf{A} &= -\mathbf{M}\mathbf{Z_{12}} + \mathbf{Z_{22}} \ . \end{aligned} \tag{14}$$

IV. OUTAGE ANALYSIS

We now derive the outage probability of the system in Fig. 1 with optimal post-detection combining. To do so, we must first identify the input to the combiner, denoted by $\mathbf{r}$ in (1). Since there is no coupling downstream from the amplifiers, $\mathbf{r}$ will simply be a scaled, sampled version of the voltage $\mathbf{V}_L$ at the amplifier output, so it suffices to place our reference point there.

A. No Matching

For simplicity, consider first the case of no matching network. After some tedious but essentially straightforward network theory, we obtain

$$\mathbf{r} = \mathbf{V}_L = \sqrt{\mathcal{E}}\mathbf{h}x + \mathbf{n} \ , \tag{15}$$

where

$$\mathbf{h} = \mathbf{D}\mathbf{C}\mathbf{h_t} \ , \tag{16}$$

$$\mathbf{n} = \mathbf{D}\mathbf{C}\left[\mathbf{n_t} - \mathbf{v_a} - (\mathbf{Z_A} + z_{cor}\mathbf{I})\mathbf{i_a}\right] + (\mathbf{I} - \mathbf{D})\mathbf{v_d}, \tag{17}$$

$\mathbf{h_t}$ and $\mathbf{n_t}$ are given in (9), $\mathbf{v_a}$ and $\mathbf{i_a}$ are the amplifier noise voltages and currents, $\mathbf{v_d}$ is the downstream noise and

$$\mathbf{C} = z_{21}(\mathbf{Z_A} + z_{11}\mathbf{I})^{-1} \tag{18}$$

$$\mathbf{D} = z_L\left[(z_L + z_{22})\mathbf{I} - z_{12}\mathbf{C}\right]^{-1} \ . \tag{19}$$

From (16), we see

$$\mathbf{\Sigma_h} = \mathbf{D}\mathbf{C}\mathbf{\Sigma_{h_t}}\mathbf{C}^H\mathbf{D}^H \ . \tag{20}$$

Recalling that $\mathbf{n_t} \sim \mathcal{CN}(\mathbf{0}, \mathbf{\Sigma_{n_t}})$, $\mathbf{v_a} \sim \mathcal{CN}(\mathbf{0}, 4kT_0Br_a\mathbf{I})$, $\mathbf{i_a} \sim \mathcal{CN}(\mathbf{0}, 4kT_0Bg_a\mathbf{I})$ and $\mathbf{v_d} \sim \mathcal{CN}(\mathbf{0}, 4kT_0Br_d\mathbf{I})$ are mutually independent, we conclude the noise covariance is

$$\begin{aligned} \frac{1}{4kT_0B}\mathbf{\Sigma_n} &= \mathbf{D}\mathbf{C}\left[\frac{1}{2}(\mathbf{Z_A} + \mathbf{Z_A^H}) + r_a\mathbf{I} \right. \\ &\quad \left. + g_a(\mathbf{Z_A} + z_{cor}\mathbf{I})(\mathbf{Z_A} + z_{cor}\mathbf{I})^H\right]\mathbf{C}^H\mathbf{D}^H \\ &\quad + r_d(\mathbf{I} - \mathbf{D})(\mathbf{I} - \mathbf{D})^H \ . \end{aligned} \tag{21}$$

Combining (20) and (21), we can now calculate the outage probability (7) from the eigenvalues of the *SNR matrix* $\mathbf{\Sigma} \equiv \mathcal{E}\mathbf{\Sigma_h}\mathbf{\Sigma_n}^{-1}$. If $\mathbf{DC}$ is nonsingular (it usually is), the form of this matrix can be simplified by observing

$$\mathbf{\Sigma_h}\mathbf{\Sigma_n}^{-1} = (\mathbf{DC})\mathbf{\Sigma_{h_t}}\mathbf{\Sigma_{\tilde{n}_t}^{-1}}(\mathbf{DC})^{-1} \tag{22}$$

where

$$\begin{aligned} \frac{1}{4kT_0B}\mathbf{\Sigma_{\tilde{n}_t}} &= \frac{1}{2}(\mathbf{Z_A} + \mathbf{Z_A^H}) + r_a\mathbf{I} + r_d\mathbf{G}\mathbf{G}^H \\ &\quad + g_a(\mathbf{Z_A} + z_{cor}\mathbf{I})(\mathbf{Z_A} + z_{cor}\mathbf{I})^H \\ \mathbf{G} &= (\mathbf{DC})^{-1}(\mathbf{I} - \mathbf{D}) \\ &= \frac{z_{22}}{z_{21}z_L}\left[\mathbf{Z_A} + \frac{(z_{11}z_{22} - z_{12}z_{21})}{z_{22}}\mathbf{I}\right] \end{aligned} \tag{23}$$

Intuitively, $\mathbf{\Sigma_{\tilde{n}_t}}$ represents the noise covariance that would result if all of the system noise were represented by an equivalent noise voltage across the antenna array.

Since the right side of (22) is a similarity transformation, the eigenvalues of $\mathbf{\Sigma_{h_t}}\mathbf{\Sigma_{\tilde{n}_t}^{-1}}$ are not changed by the transformation. We can therefore take the SNR matrix to be

$$\begin{aligned} \mathbf{\Sigma} &= \frac{\mathcal{E}}{4kT_0B}\mathbf{\Sigma_{h_t}}\left[\frac{1}{2}(\mathbf{Z_A} + \mathbf{Z_A^H}) + r_a\mathbf{I} + r_d\mathbf{G}\mathbf{G}^H \right. \\ &\quad \left. + g_a(\mathbf{Z_A} + z_{cor}\mathbf{I})(\mathbf{Z_A} + z_{cor}\mathbf{I})^H\right]^{-1} . \end{aligned} \tag{24}$$

B. Matching

Now suppose a matching network is inserted between the antennas and amplifiers, as shown in Fig. 1. From (14), it follows that (24) still applies with $\mathbf{\Sigma_{h_t}}$ replaced by $\mathbf{M}\mathbf{\Sigma_{h_t}}\mathbf{M}^H$ and $\mathbf{Z_A}$ replaced by $\mathbf{Z}'_\mathbf{A}$. The SNR matrix is therefore

$$\begin{aligned} \mathbf{\Sigma} &= \frac{\mathcal{E}}{4kT_0B}\mathbf{M}\mathbf{\Sigma_{h_t}}\mathbf{M}^H\left[\frac{1}{2}(\mathbf{Z}'_\mathbf{A} + \mathbf{Z}'^H_\mathbf{A}) + r_a\mathbf{I} \right. \\ &\quad \left. + r_d\mathbf{G}'\mathbf{G}'^H + g_a(\mathbf{Z}'_\mathbf{A} + z_{cor}\mathbf{I})(\mathbf{Z}'_\mathbf{A} + z_{cor}\mathbf{I})^H\right]^{-1} \end{aligned} \tag{25}$$

where $\mathbf{G}'$ is given by (23) with $\mathbf{Z_A}$ replaced by $\mathbf{Z}'_\mathbf{A}$.

V. NUMERICAL RESULTS

In the previous section, we derived a general outage probability formula that applies to any narrowband Rayleigh fading model, antenna array, matching network, front-end amplifiers and downstream noise. In this section, we numerically evaluate the outage probability for several specific examples.

We consider a uniform linear array of $M = 2$ or 4 half-wavelength dipoles spaced a distance d apart. Each dipole has radius $10^{-3}\lambda$, where λ is the signal wavelength. The incident electric field is a superposition of $N = 32$ vertically-polarized plane waves with i.i.d. phases uniformly distributed on $(0, 2\pi)$. The angles-of-arrival (AOA) of the plane waves, $\phi_0, \ldots, \phi_{N-1}$, are uniformly spaced in azimuth from 0 to 2π. Under these conditions, the open-circuit fading path gains (9) are approximately Gaussian with correlation matrix

$$[\mathbf{\Sigma_{h_t}}]_{nm} = \sum_{k=0}^{N-1} g_n(\phi_k)g_m^*(\phi_k)e^{j2\pi(n-m)\frac{d}{\lambda}\cos\phi_k} \ , \tag{26}$$

where $g_n(\phi)$ is the open-circuit voltage induced in the n^{th} antenna by a zero-phase plane wave with AOA ϕ, normalized so that $\sum_k |g_n(\phi_k)|^2 = 1$ for an isolated dipole.

For omnidirectional antennas (i.e., $g_n(\phi)$ is constant) this expression converges for large N to Clarke's formula [21]:

1930-529X/07/$25.00 © 2007 IEEE
This full text paper was peer reviewed at the direction of IEEE Communications Society subject matter experts for publication in the IEEE GLOBECOM 2007 proceedings.

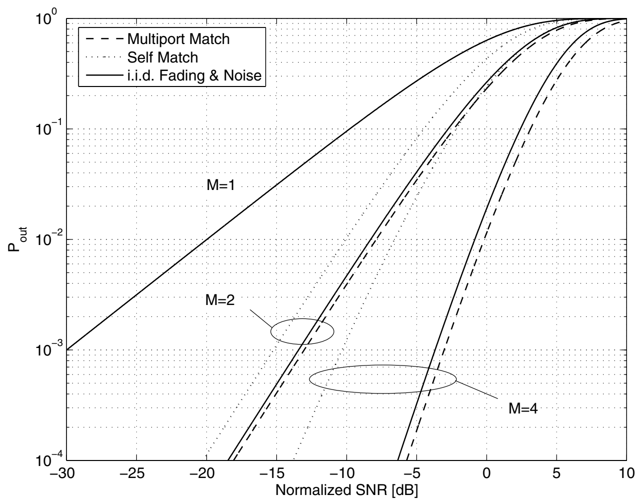

Fig. 3. Outage probability for multiport and self matching, $d = 0.1\lambda$

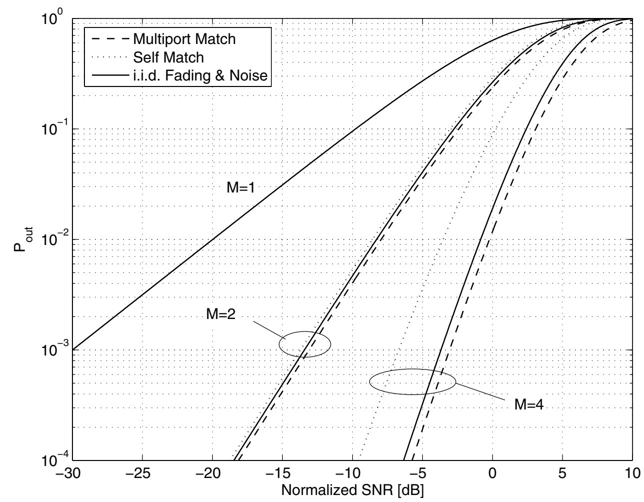

Fig. 4. Outage probability for multiport and self matching, $d = 0.2\lambda$

$J_0(2\pi|n-m|d/\lambda)$, where $J_0(x)$ is the zeroth-order Bessel function of the first kind. While the elements of an array of infinitesimally thin wire dipoles are omnidirectional, assuming so for dipoles of finite thickness may be inaccurate. For this reason we calculated $g_n(\phi)$ numerically using the Numerical Electromagnetics Code (NEC) [22], a popular Method-of-Moments based electromagnetic solver. NEC was also used to find the array impedance matrix $\mathbf{Z_A}$, yielding more accurate results than the thin-wire approximation.[5]

The amplifier selected for this study is a low-cost SiGe LNA [23] designed for use in the cellular band. In high-gain mode with $R_{\text{bias}} = 510\ \Omega$ and $f = 900$ MHz, its impedance matrix and Rothe-Dahlke noise parameters are:

$$\begin{bmatrix} z_{11} & z_{12} \\ z_{21} & z_{22} \end{bmatrix} = \begin{bmatrix} 35.7\angle -82.0^{\text{o}} & 2.74\angle 91.8^{\text{o}} \\ 325\angle 119^{\text{o}} & 46.1\angle -23.3^{\text{o}} \end{bmatrix} \Omega$$

$$r_a = 9.45\ \Omega, \quad g_a = 3.24 \text{ mS}, \ z_{cor} = 35.3\angle -114^{\text{o}}\ \Omega$$

This amplifier is approximately unilateral ($z_{21} \gg z_{12}$) and the minimum noise figure is quite low (1.04 dB), ideal characteristics for front-end amplifiers. In practice the noise figure may be slightly higher due to impedance mismatch and other implementation issues, but still low enough (typically a few dBs) that amplifier noise cannot be regarded as dominant.

The load impedance is taken as the conjugate of the amplifier output impedance, i.e., $z_L = z_{22}^*$. In this initial study we neglect downstream noise, so $r_d = 0$. For the amplifier and matching networks used in this example, the elements of $\mathbf{G}'\mathbf{G}'^H$ are typically two orders of magnitude less than the antenna and amplifier noise contributions in (25). Therefore, neglecting downstream noise should not significantly affect results for moderate values of r_d. The more general case of non-negligible downstream noise will be considered elsewhere.

[5]There is a significant difference in the mutual impedance calculated using the thin-wire approximation and NEC for closely coupled dipoles; see Figs. 8.21 and 8.22 in [15].

We now evaluate outage for two matching networks considered in [10]. In *optimal multiport matching* for minimum noise figure, the network (14) is chosen so that $\mathbf{Z}'_{\mathbf{A}} = z_{opt}\mathbf{I}$, where z_{opt} is the source impedance (13) that minimizes the noise factor F. One network that accomplishes this task is

$$\begin{bmatrix} \mathbf{Z_{11}} & \mathbf{Z_{12}} \\ \mathbf{Z_{21}} & \mathbf{Z_{22}} \end{bmatrix} = \begin{bmatrix} \frac{1}{2}\left(\mathbf{Z}_{\mathbf{A}}^H - \mathbf{Z_A}\right) & -j\mathbf{U}\left(r_{opt}\mathbf{\Lambda}\right)^{\frac{1}{2}} \\ -j\left(r_{opt}\mathbf{\Lambda}\right)^{\frac{1}{2}}\mathbf{U}^H & jx_{opt}\mathbf{I} \end{bmatrix} \quad (27)$$

where $\frac{1}{2}\left(\mathbf{Z_A} + \mathbf{Z}_{\mathbf{A}}^H\right) = \mathbf{U\Lambda U}^H$, $\mathbf{\Lambda}$ is diagonal and $\mathbf{U}$ is a unitary matrix. Applying (25) for multiport matching, the normalized SNR matrix is

$$\frac{1}{\sigma^2}\mathbf{\Sigma} = 2r_s\left(\mathbf{Z_A} + \mathbf{Z}_{\mathbf{A}}^H\right)^{-1}\mathbf{\Sigma_{h_t}}\ , \quad (28)$$

where $\sigma^2 = \mathcal{E}/4kT_0BF_{min}r_s$ is the SNR of a single-antenna system and r_s is the real part of the antenna self-impedance.

The matching network (27) can be difficult to realize in practice. A simpler, suboptimum strategy is to apply to each receive antenna the two-port matching network that achieves the minimum noise figure for that antenna in isolation. This is called *self matching* for minimum noise figure and is accomplished by the network

$$\begin{bmatrix} \mathbf{Z_{11}} & \mathbf{Z_{12}} \\ \mathbf{Z_{21}} & \mathbf{Z_{22}} \end{bmatrix} = \begin{bmatrix} -jx_s\mathbf{I} & -j\sqrt{r_{opt}r_s}\mathbf{I} \\ -j\sqrt{r_{opt}r_s}\mathbf{I} & jx_{opt}\mathbf{I} \end{bmatrix}. \quad (29)$$

For self-matching, the normalized SNR matrix is

$$\begin{aligned} \frac{1}{\sigma^2}\mathbf{\Sigma} \quad = \quad & r_sF_{min}\mathbf{M\Sigma_{h_t}M}^H\Bigg[\frac{1}{2}(\mathbf{Z}'_{\mathbf{A}} + \mathbf{Z}'^H_{\mathbf{A}}) + r_a\mathbf{I} \\ & +g_a(\mathbf{Z}'_{\mathbf{A}} + z_{cor}\mathbf{I})(\mathbf{Z}'_{\mathbf{A}} + z_{cor}\mathbf{I})^H\Bigg]^{-1}. \quad (30) \end{aligned}$$

If the antenna spacing is sufficiently large so that coupling may be neglected (30) reduces to $\mathbf{\Sigma} = \sigma^2\mathbf{\Sigma_{h_t}}$.

The outage probability for multiport and self matching and $M = 2, 4$ are shown in Figs. 3 and 4 for antenna separations of $d = 0.1\lambda$ and 0.2λ, respectively. Included for comparison are the outage curves for i.i.d. fading and noise (8). For two

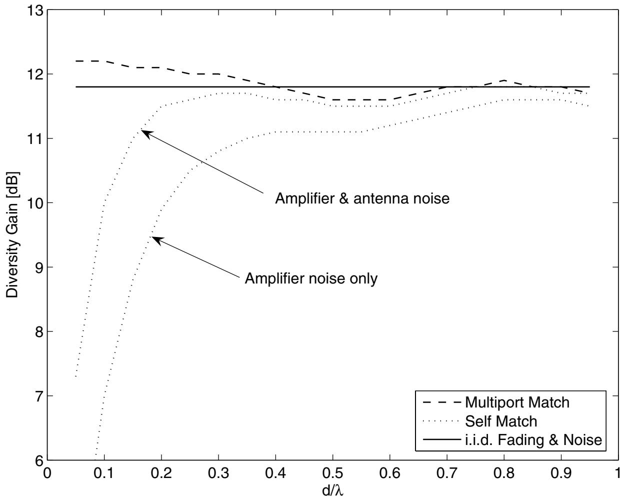

Fig. 5. Diversity gain at 1% outage for M=2 with multiport and self matching.

antennas separated by $d = 0.1\lambda$, multiport matching is slightly better than the i.i.d. case; however, there is a penalty of ~ 2 dB for self matching. This penalty is almost completely eliminated by increasing d to 0.2λ, which is interesting since the antennas are still strongly coupled at this distance. Note that the penalty for self matching is significantly increased for $M = 4$. In particular, the benefit of using more than two antennas is significantly less with self matching than multiport matching.

Finally, we examine the impact of different noise sources on the diversity gain, defined as the difference in SNR between the $M = 2$ and $M = 1$ outage curves at a fixed probability. In Fig. 5 the diversity gain at 1% outage is shown for [6] $0.05\lambda \leq d \leq \lambda$ and two dual diversity systems: One with both antenna and amplifier noise (as in Figs. 3 and 4), and one in which amplifier noise alone dominates. For multiport matching, there is no difference in performance between the two systems and little difference from the i.i.d. fading and noise case. For self matching, however, observe that amplifier noise leads to significantly worse performance than antenna and amplifier noise. This is due to the fact that the antenna noise component in (30) remains highly correlated for self matching, and optimal combining can exploit this correlation to improve the gain. The effect of noise correlation may also be seen by considering a case in which antenna noise is dominant. For any matching network the SNR matrix in this case reduces to (28), so the diversity gain would be identical to the multiport matching plot in Fig. 5.

We conclude that different noise sources can impact performance in profoundly different ways. This example illustrates the importance of clearly identifying and modeling the distinct sources of noise in coupled multiple-antenna systems.

VI. Conclusion

We presented a diversity receiver model that includes the most common sources of noise. The outage probability of the optimal diversity receiver was derived in terms of the output noise correlation, which in turn was shown to depend on receiver noise sources, antenna coupling, the front-end amplifiers and matching network. We further illustrated by example that different noise sources can impact performance in profoundly different ways.

[6] The azimuthally uniform current distribution assumption employed in NEC may be less reliable at antenna separations smaller than 0.05λ.

References

[1] W. C. Y. Lee, "Mutual coupling effect on maximum-ratio diversity combiners and application to mobile radio," *IEEE Trans. Commun. Technol.*, vol. COM-18, pp. 779 - 791, Dec. 1970.

[2] J. H. Winters, "Optimum combining in digital mobile radio with cochannel interference," *IEEE Trans. Veh. Technol.*, vol VT-33, pp. 144-155, Aug. 1984.

[3] G. J. Foschini and M. J. Gans, "On limits of wireless communications in a fading environment when using multiple antennas," *Wireless Personal Communications*, vol. 6, pp. 311-335, 1998.

[4] T. S. Svantesson and A. Ranheim, "Mutual coupling effects on the capacity of multielement antenna systems," in *Proc. IEEE ICASSP*, 2001, pp. 2485-2488.

[5] C. Waldschmidt, J. v. Hagen, and W. Wiesbeck, "Influence and modeling of mutual coupling in MIMO and diversity systems," in *Proc. IEEE AP-S Inter. Symp.*, 2002, pp. 190-193.

[6] R. Janaswamy, "Effect of element mutual coupling on the capacity of fixed length linear arrays," *Antennas Wireless Propag. Lett.*, vol. 1, pp. 157-160, 2002.

[7] B. Clerckx et al, "Mutual coupling effects on the channel capacity and the space-time processing of MIMO communication systems," in *Proc. IEEE ICC*, 2003, pp. 2638-2642.

[8] J. W. Wallace and M. A. Jensen, "Mutual coupling in MIMO wireless systems: A rigorous network theory analysis," *IEEE Trans. Wireless Commun.*, vol. 3, pp. 1317-1325, Jul. 2004.

[9] X. Li and Z. Nie, "Mutual coupling effects on the performance of MIMO wireless channels," *IEEE Antennnas Wireless Propag. Lett.*, vol. 3, pp. 344-347, 2004.

[10] M. L. Morris and M. A. Jensen, "Improved network analysis of coupled antenna diversity performance," *IEEE. Trans. Wireless Commun.*, vol. 4, pp. 1928-1934, Jul. 2005.

[11] M. J. Gans, "Channel capacity between antenna arrays – Part I: Sky noise dominates," *IEEE Trans. Commun.*, vol. 54, pp. 1586-1592, Sep. 2006.

[12] M. J. Gans, "Channel capacity between antenna arrays – Part II: Amplifier noise dominates," *IEEE Trans. Commun.*, vol. 54, pp. 1983-1992, Nov. 2006.

[13] D. G. Brennan, "Linear diversity combining techniques," *Proc. IRE*, vol. 47, pp. 1075-1102, Jun. 1959.

[14] J. E. Hudson, *Adaptive Array Principles*. London: IEE Press, 1981.

[15] C. A. Balanis, *Antenna Theory: Analysis and Design*, 3rd ed. New York: Wiley, 2005.

[16] W. R. Bennett, *Electrical Noise*. New York: McGraw Hill, 1960.

[17] R. Q. Twiss, "Nyquist's and Thevenin's theorems generalized for nonreciprocal linear networks," *J. Applied Physics*, vol. 26, pp. 599-602, May 1955.

[18] H. Rothe and W. Dahlke, "Theory of noisy fourpoles," *Proc. IRE*, vol. 44, pp. 811-818, Jun. 1956.

[19] H. A. Haus and R. B. Adler, *Circuit Theory of Linear Noisy Networks*. New York: Wiley, 1959.

[20] D. M. Pozar, *Microwave Engineering*, 3rd ed. New York: Wiley, 2005.

[21] R. H. Clarke, "A statistical theory of mobile-radio reception," *Bell Syst. Tech. J.*, vol. 47, pg 957-1000, Jul. 1968.

[22] G. J. Burke and A. J. Poggio, "Numerical Electromagnetics Code (NEC) – Method of moments," Tech. Doc. 11, Naval Ocean Systems Center, San Diego, CA, Jan. 1981.

[23] http://datasheets.maxim-ic.com/en/ds/MAX2642-MAX2643.pdf